Dynamic Force Spectroscopy of Photoswitch-Modified DNA

Esha Sengupta,[†] Yunqi Yan,[†] Xin Wang,[†,‡] Keiko Munechika,[†,§] and David S. Ginger[†,*]

[†]Department of Chemistry, University of Washington, Seattle, Washington 98195, United States, [‡]Molecular & Cell Biology Division, Life Technologies, Eugene, Oregon 97402, United States, and [§]Molecular Foundry, Lawrence Berkeley National Laboratory, One Cyclotron Road, Berkeley, California 94720, United States

ABSTRACT We apply a combination of photoswitch-modified DNA and AFM-based pulling measurements to study the force-induced melting of double-stranded DNA in the unzipping geometry. We measure the differences in peak rupture force for azobenzene-modified DNA, as the incorporated azobenzenes are photoswitched reversibly between the *trans* and the *cis* form. Fitting our rupture force *versus* loading rate data, we obtain off rate (k_{off}) at zero force values in the range of ~10 s^{-1}. We show that the change in peak rupture force and k_{off} induced by destabilizing the DNA duplex depends on the position of the destabilizing azobenzene photoswitch relative to the force-loading site. When the azobenzenes are proximal to the unzipping end, the decrease in peak force and k_{off} upon azobenzene photoisomerization is significantly larger than when the azobenzene is distal to the site of force loading. We interpret these results as experimental evidence supporting the picture that the destabilization of a double-stranded DNA by a photoswitch isomerization is localized to a small bubble around the photoswitch.

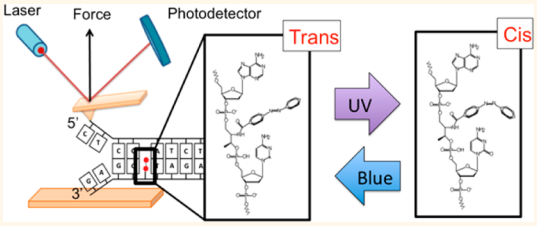

KEYWORDS: dynamic force spectroscopy · azobenzene-modified DNA · reversible photoswitching · position-dependent rupture force

DNA melting is the process by which double-stranded DNA separates into two single strands of DNA. This process is of fundamental importance to DNA replication[1] and transcription[2] and is a key step in PCR-based applications, nanodevices,[3−5] DNA sensing technologies,[6] and genetic medicine.[7] Despite years of study, interesting questions such as the mechanical properties of DNA[8] and unzipping mechanism of DNA duplexes remain active topics of research.[9−12]

DNA melting is commonly initiated by an increase in temperature, decrease in ionic strength, or, in some cases, mechanical loading with an applied force.[13−16] However, the commercial availability of azobenzene-modified DNA[17−20] has added illumination with light as a new means by which DNA melting can be controlled *via* external stimulus.[21−24] As a result, phototriggered DNA melting is now being used for applications ranging from drug delivery[25] and biosensing to nanoscale motors and energy harvesting.[18−20,22,23,26] However, the unzipping mechanisms of unmodified DNA remain topics of open investigation, and the physicochemical properties of photoswitch-modified DNA have only begun to be studied.

Single-molecule pulling measurements, often conducted using an atomic force microscope[27−34] or optical tweezers, have played a critical role in our understanding of the thermodynamics and kinetics of biomolecular processes and interactions, including the force-induced melting of DNA. Such dynamic force spectroscopy (DFS) experiments can be used to measure the pico-Newton scale forces associated with unbinding of even short oligonucleotides (20−100 nucleotides)[35] and have been used to obtain thermodynamic data for base pairing in the limit of slow force loading.[36,37] Although challenges with separating specific from nonspecific interactions exist,[37] at faster force-loading rates, analysis of DFS data can be used to extract kinetic parameters such as individual k_{off} rates for the binding events under investigation.[37,38]

Here, we employ azobenzene-modified DNA[17,39,40] in DFS experiments designed to study both the specific properties of azobenzene-modified sequences as well as the more general question of how short DNA sequences unzip under force loading. We show that the reversible photoswitching of the azobenzenes can be detected as reversible changes in the force-induced unzipping behavior of the

* Address correspondence to ginger@chem.washington.edu.

Received for review December 10, 2013 and accepted February 6, 2014.

Published online February 06, 2014
10.1021/nn406334b

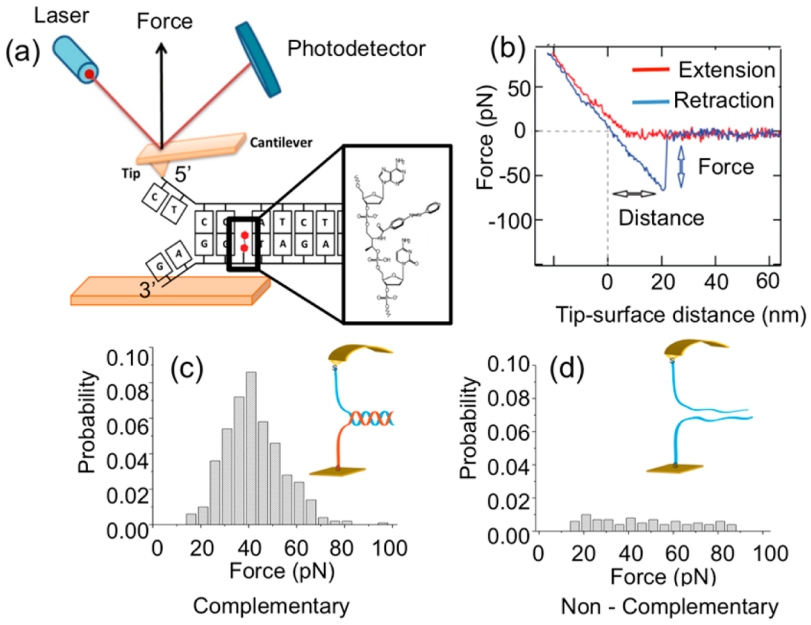

Figure 1. (a) Schematic of the experimental setup. One DNA strand (free of azobenzenes) is functionalized onto the cantilever tip, and the other strand (modified with azobenzenes) is anchored to the substrate. (b) Typical force−distance (FD) curve showing the rupture force between the DNA duplex. Histograms of the rupture forces between (c) complementary and (d) noncomplementary strands of DNA.

modified double-stranded DNA. By fitting our data to extract the k_{off}, we show that the effect of the azobenzene photoswitch[41] on the unzipping is sensitive to the azobenzene position within the sequence in a manner that is consistent with theoretical predictions.

RESULTS AND DISCUSSION

We use azobenzenes covalently bonded to the DNA sugar−phosphate backbone *via* a D-threoninol group as phototriggers (Figure 1a, inset) using the commercial Asanuma chemistry.[17] In the *trans* form, incorporation of an azobenzene into the DNA backbone stabilizes the DNA duplex *via* π-stacking interactions.[17] However, upon exposure to UV (~350 nm) light, the *trans*-azobenzene undergoes photoisomerization to *cis*-azobenzene (with a quantum yield dependent on the local sequence[40]). The *cis*-azobenzene destabilizes the double strand and can lead to subsequent melting of the DNA. While *cis*-azobenzene is metastable with a lifetime of many hours at room temperature, blue light (>400 nm) can be used to quickly photoisomerize *cis*-azobenzene back to *trans*-azobenzene, providing a fully reversible trigger that can modulate the hybridization and melting properties of the DNA.

Figure 1a shows our general experimental scheme. We performed DFS by bringing tips functionalized with single-strand DNA (ssDNA) into contact with substrates functionalized with complementary ssDNA and retracting at various rates. We chose sequences so that our pulling experiments would utilize the "unzipping" geometry.

We first performed control experiments to verify that our functionalization and pulling protocols allowed us to measure rupture forces due to the binding of the complementary DNA sequences rather than nonspecific interactions. For these controls, we functionalized a Au-coated AFM cantilever tip with a 5′-thiolated DNA strand (5′-SH-T_{30}GACTCCATCTGAACTAACG-3′) (see Methods). We then functionalized a Au-coated substrate with the complementary DNA strand (3′-SH-T_{30} GACTGGTAGACTT-GATTGC-5′, T_m is 58.6 0.6 °C when hybridized with the partially complementary DNA sequence used in these experiments; see Supporting Information).

Figure 1b shows a typical "good" force−distance curve obtained for this complementary DNA pair using a cantilever (Asylum research BL-RC-150VB, force constant k = 0.006 N/m) at a loading rate of 3 nN/s. The red line indicates extension/approach, and the blue line indicates the retraction of the cantilever, showing a typical good unbinding event. We acquired several hundred pulling curves on Au surfaces functionalized with complementary and noncomplementary DNA, and we analyzed histograms for the rupture forces. Figure 1c,d shows the resulting histograms of rupture forces obtained on the complementary and noncomplementary surfaces, respectively. The complementary sequences give a much larger percentage of successful pulls (60% for complementary *vs* 15% for noncomplementary), and the complementary−DNA surface exhibits a rupture force peak at roughly ~30−40 pN. In contrast, we observe no force peak for the noncomplementary DNA—only a flat (random) distribution for the (far fewer) pulling events that passed through the analysis algorithm on the noncomplementary control. Although we reserve an in-depth analysis of peak rupture force *versus* loading-rate data for the photoswitchable DNA data below, we note that the peak rupture force near ~40 pN is consistent with typical unbinding data in the unzipping geometry for

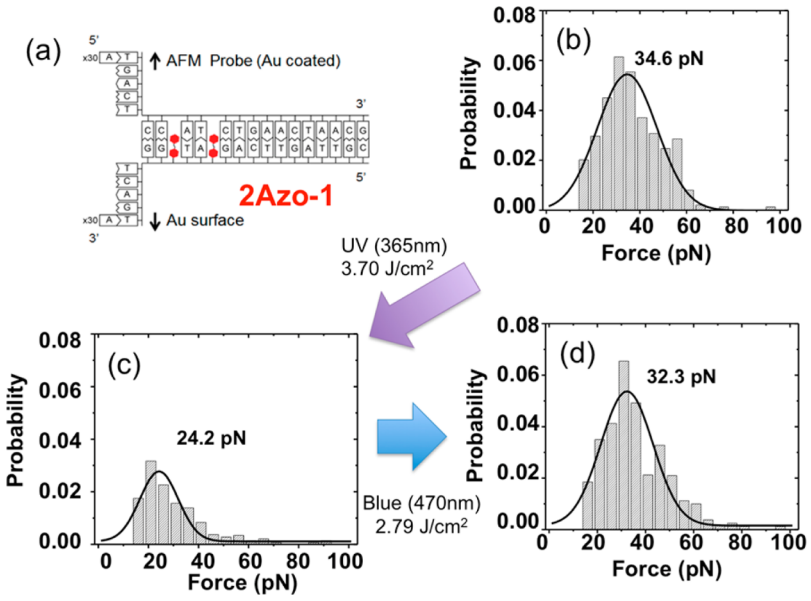

Figure 2. (a) DNA strands modified with two azobenzene groups (sequence named as "2Azo-1") used for the pulling experiment. Double-stranded DNA shows a peak rupture force at (b) 34.6 pN before UV irradiation and a reduced force at (c) 24.2 pN after UV irradiation; (d) duplex recovers a peak rupture force back to 32.3 pN (along with an increase in "good" pulls) after subsequent blue irradiation.

comparable length DNA sequences in the literature.[42] Having confirmed that our experimental protocols behave as expected with ordinary DNA, we thus turn to focus on more novel experiments with photoswitchable azobenzene-modified oligonucleotides.

For these experiments, as shown in Figure 2a, we again functionalized the AFM cantilever tip with the same 5′-thiolated DNA strand (5′-SH-T_{30} GACTCCATCT-GAACTAACG-3′) (see Methods). However, we functionalized the Au-coated substrate with the complementary DNA strand modified with azobenzenes (3′-SH-T_{30} GACTGGXTAXGACTTGATTGC-5′, named 2Azo-1, T_m is 60.0 ± 0.0 °C when hybridized with the partially complementary DNA sequence used in these experiments; see Supporting Information). Here X denotes an azobenzene molecule that, when exposed to UV light, photoisomerizes to *cis*-azobenzene and destabilizes the duplex.

We measured force-pulling curves at a loading rate of 3 nN/s and plotted the resulting histogram, fitting it with a Gaussian to determine the most probable rupture force (34.6 pN, Figure 2). Next, we illuminated the substrate with 365 nm UV light of an intensity of 342.5 μW/cm^2 to obtain a total exposed dose of 3.7 J/cm^2 (which is sufficient to achieve a photostationary state of predominantly *cis*-form azobenzene).[40] We then irradiated the substrate, again, this time with 470 nm blue light with an intensity of 387.5 μW/cm^2 for a total exposed dose of 2.79 J/cm^2. Figure 2c plots the peak rupture force data after the UV irradiation, showing that the most likely rupture force has decreased from 34.6 to 24.2 pN. Both this decrease in rupture force and the decrease in the fraction of "good" pulls (from 60% for *trans* to 25% for *cis*) are qualitatively consistent with the expected destabilization of the DNA double strands by the *cis*-form azobenzenes incorporated into the substrate-bound oligonucleotides. Importantly, Figure 2d shows that, following irradiation with blue light to return the azobenzenes to *trans* form, the peak rupture force histogram returns almost completely to its preirradiation behavior. This result thus confirms that the photoswitching is reversible and provides further evidence that the rupture forces we are measuring are associated with hybridized azobenzene-modified oligonucleotides.

Having verified the ability of azobenzene photoswitches to reversibly modulate the peak rupture force histograms obtained from pulling experiments on azobenzene-modified DNA, we next turn to analyze the effect of photoswitching on DNA binding more quantitatively. The classic method to extract unbinding kinetics data from DFS experiments is by measuring the peak rupture force as a function of loading rate.[37,43]

In this context, the Bell–Evans model has been widely used to describe the trend of the unbinding forces as a function of the loading rates.[36] The Bell–Evans model is given by eq 1:

$$F = \frac{k_B T}{x_t} \ln\left(\frac{r x_t}{k_{off} k_B T}\right) \quad (1)$$

where r is the loading rate (N/s), x_t is the distance between the bound and the transition state along the direction of the applied force, k_{off} is the dissociation rate, k_B is the Boltzmann constant, and T is the temperature. As seen by the functional form of eq 1, this model predicts that the rupture force of a single bond varies as the logarithmic of the loading rate. This model assumes that, at low loading rates, the thermal energy overcomes the

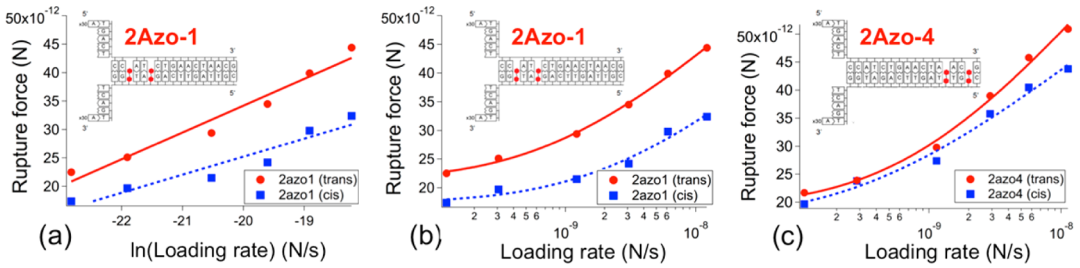

Figure 3. (a) Rupture force is plotted as a function of natural log of force-loading rate for DNA strands modified with two azobenzenes (red dots, *trans* form; blue squares, *cis* form) proximal to the unzipping end (2Azo-1). The data are fitted with Bell−Evans model (straight and dashed lines). (b) Same data from (a) are fitted with the Friddle model. (c) Data of DNA strands modified with two azobenzenes distal to the unzipping end (2Azo-4) are fitted with the Friddle model.

activation barrier and therefore less external force is required to rupture the bonds.

As suggested by the form of eq 1, Figure 3a plots our peak rupture force data *versus* the natural logarithm of the force-loading rate taken for the same 2Azo-1 sequences studied in Figure 2. Traces are shown both before UV irradiation (*trans* form, red circles) and after UV irradiation (*cis* form, blue squares). As expected, the peak rupture force decreases at all loading rates after the azobenzenes are switched into the *cis* form. The straight lines in Figure 3a are fits to the Bell−Evans model. The k_{off} value calculated for the *trans* data from this model is $0.33 \pm 0.11\ s^{-1}$. On irradiating the sample with UV light for 3 h, we observe a decrease in the measured peak rupture force at each loading rate (blue squares). For the *cis* data, the k_{off} value obtained on fitting the curve with the Bell−Evans model (blue dashed line) is nearly equal within uncertainty at $0.22 \pm 0.08\ s^{-1}$.

The Bell−Evans fits are unsatisfactory in two ways. First, it is clear that the experiments in Figure 3a are not fit well by straight line as predicted by eq 1. Second, as a consequence of the poor fits, the k_{off} extracted for the *cis*-form azobenzene is the same as or lower than that of the *trans*-form azobenzene. While it is possible that the *cis*-form azobenzene both destabilizes the DNA double strand and decreases k_{off}, we find this conclusion unlikely.

A number of authors have pointed out circumstances in which a simple fitting to the Bell−Evans model might fail.[44,45] In particular, the Bell−Evans model ignores the asymmetric behavior of the rupture forces at high loading rates, as suggested by Dudko *et al.*,[45] as well as the possibility of more than a single binding of interacting molecules.[37] Thus, we analyzed our data using a generalized model proposed by Friddle, Noy, and DeYoreo.[38,46] Their model explains the nonlinearity in the force spectra as a consequence of re-forming of a single bond at slow loading rates as well as asynchronous fluctuations of several independent interactions that comprise a multivalent attachment. Thus, their model takes into account the harmonic potential of the cantilever and the number of bonds formed between the probe and the substrate (N).

The force spectrum from this model is given by eqs 2 and 3:[38]

$$\langle f \rangle_N = f_{eq} + N\frac{k_B T}{x_t}\exp\left(\frac{N}{R\left(\frac{f_{eq}}{N}\right)}\right) E_1\left(\frac{N}{R\left(\frac{f_{eq}}{N}\right)}\right) \quad (2)$$

$$R\left(\frac{f_{eq}}{N}\right) = \frac{r x_t}{k_{off}\left(\frac{f_{eq}}{N}\right) k_B T} \quad (3)$$

where

$$k_{off}(f) = k_{off}^0 \exp\left[\beta\left(f x_t - \frac{1}{2}k_c x_t^2\right)\right] \quad (4)$$

where k_{off}^0 is the intrinsic unbinding rate at zero force, k_c is the spring constant of the cantilever, f_{eq} is a force given by $f_{eq} = (2k_c \Delta G_{bu})^{1/2}$, $E_1(z) = \int_z^\infty (e^{-s}/s)ds$, r is the loading rate, x_t is position of the energy barrier, and ΔG_{bu} is the free energy of the bond relative to the free cantilever. Using this model, they described a vast number of nonlinear spectra collected from vastly dissimilar intermolecular systems. We verified that our rupture force *versus* loading rate data was dependent upon the cantilever spring constant as predicted in the above equations (see Supporting Information Figure S1).

Figure 3b replots the peak rupture force *versus* loading rate data taken for the 2Azo-1 sequences for fitting with the Friddle model (solid lines). The red circles indicate the rupture forces obtained for the azobenzenes in their *trans* form, whereas the blue squares indicate *cis*-form azobenzene after UV irradiation. For the *trans*-azobenzene (solid red line), the k_{off} value extracted from the Friddle model is $5.98 \pm 2.54\ s^{-1}$ (for full fitting details, see Supporting Information Figure S3). For the *cis*-azobenzene (blue dashed line), the best fit k_{off} value is $22.6 \pm 2.96\ s^{-1}$. Use of the Friddle model thus not only reproduces the curvature of our data at low loading rates but also now yields k_{off} trends that make sense. The k_{off} rate for destabilized DNA with *cis*-form azobenzene is now higher than the corresponding k_{off} for *trans*-form azobenzene strands.

Quantitatively, these k_{off} values are surprisingly larger than might be expected for an all-at-once type force-induced bond rupture event or from conventional measurements of sequence-dependent DNA unbinding rates. For similar sequences, k_{off} from experiments such as SPR[47] and AFM pulling measurements in a shear geometry[42] would be expected to show much smaller values ($\approx 10^{-3}$ s^{-1}). Indeed, our measured k_{off} rates on the order of ~ 10 s^{-1} would more likely be associated with melting of short 4–5 base sequences.[42] We propose that this discrepancy can be reconciled by considering the force-biased geometry of our experiment (unzipping *vs* a shear loading) experiments. In the unzipping process, a number of theory papers have argued that, as might be expected from intuition, the applied force is distributed over a small number of bases in an unzipping geometry.[48,49] Thus, one plausible interpretation of a k_{off} of $\sim 1-10$ s^{-1} is that the applied force is felt locally by the first ~ 4 bases in the azobenzene-modified DNA. Consistent with this interpretation, one finds reports of rates of $\sim 1-10$ s^{-1} for force-induced unzipping of DNA in a limited number of experiments.[50]

Finally, we consider the effect of the azobenzene position on force-induced DNA melting in the unzipping geometry. We functionalized the Au-coated surface with a slightly different azobenzene-modified DNA that has two azobenzenes incorporated farther from the unzipping end (3′-SH-T_{30} GACTGGTAGACTTGATXTGXC-5′, named 2Azo-4; T_m is 61.0 ± 0.5 °C when hybridized with the partially complementary DNA sequence used in these experiments; see Supporting Information). Figure 3c shows experimental rupture force *versus* loading rate data, along with fits to the Friddle model, for 2Azo-4, which has the azobenzene photoswitches positioned at the far end of the DNA strand, away from the unzipping point. For this sequence, we measured a much smaller change in peak rupture after the azobenzene isomerized. The fitted k_{off} value for the *trans*-azobenzene DNA (red solid line) is calculated to be 8.80 ± 4.97 s^{-1}, whereas that of the *cis* form (blue dashed line) is 3.28 ± 3.47 s^{-1}. These results are indistinguishable within the quality of the fits.

This result shows a qualitative and striking difference in the effect of photoisomerization on k_{off} between the two sequences, which is in good agreement with our rationalization of the large k_{off} values. Evidently, when the azobenzene is near the site of force loading, photoisomerization results in a significant increase in k_{off} and reduction in force required to unzip the duplex. However, when the azobenzene is farther away from the site of force loading, it exhibits a much smaller effect. We believe these results are in good qualitative agreement with theoretical predictions. Cocco *et al.* have previously predicted that DNA unzipping should begin with a transition "bubble" a few (≈ 4) bases long,[49] and Schatz and co-workers have previously computed that a local defect surrounding a photoisomerized azobenzene would create only a small region of destabilization of similar length.[51] Thus, we interpret our data as indicating that the rupture force and k_{off} rate show the largest change upon photoisomerization if the region of the duplex destabilized by photoisomerization of the azobenzene overlaps with the transition bubble at the start of the unzipping event.

CONCLUSIONS

We have performed DFS measurements on azobenzene-modified DNA. We have shown that azobenzene photoisomerization of surface-bound DNA can be used to reversibly modulate the rupture force required to unzip double-stranded DNA. Importantly, and in qualitative agreement with computational predictions, our data suggest that the position of the azobenzene within the unzipping sequence controls the magnitude of change in k_{off} rate upon azobenzene photoisomerization. We observe a significant (4×) increase in k_{off} when the azobenzene is in close proximity to the unzipping end of the DNA and a smaller difference (within experimental uncertainty) when the azobenzene is at the opposite end of the DNA. These results provide important insights into the melting kinetics of photoswitch-modified oligonucleotides that should be useful for designing photoswitch-modified sequences for specific applications. They also show that photoswitches may provide a new tool for studying classic mechanisms in DNA hybridization and melting.

METHODS

Preparation of DNA Solution. Unmodified DNA and azobenzene-modified DNA were purchased from Integrated DNA Technology (IDT Inc., IA). Aliquots of lyophilized DNA were first dissolved in water, which was deionized to 18.0 MΩ with a Millipore filtration system. A desired amount of DNA (typically 2 μM) was then resuspended in aqueous solution containing 1 mM phosphate buffer saline (PBS), 0.3 M NaCl, and 0.02% sodium azide. These prepared DNA solutions were stored at 4 °C prior to use.

Tip and Surface Modification. Au-coated Biolever (BL-RC-150VB Olympus) cantilevers were used for the force-pulling experiments. Initially, 20 μL of filtered ethanol was drop cast on the cantilever and kept for 5 min before rinsing it off and drop casting 20 μL of 1 μM DNA solution. This was kept for 15 min to functionalize the tip with DNA strands. Next, we removed the DNA solution and washed the tips with fresh 1 mM PBS buffer (0.01% SDS) twice. The tips were then backfilled with mercaptoundecanol (2 μM in PBS) for 10 min and then rinsed again with fresh PBS buffer. The functionalized cantilever tip was then left in PBS buffer (0.3 M Na^+) until use.

Freshly evaporated Au films on glass (~2 nm Cr, ~5–10 nm Au) were prepared by thermal evaporation at a base pressure of 5×10^{-7} mbar and at a deposition rate of ~0.05–0.1 nm/s.

Thirty microliters of azo-modified DNA solution (2 μM) was drop cast. Since the clean Au surface is hydrophilic, the solution tends to spread rapidly. A single well (SecureSeal Hybridization Chamber, GraceBio Laboratories) was gently pressed and then removed to create a hydrophobic barrier. The DNA solution was kept on the substrate for 1 h. Next, the substrate was rinsed thoroughly with 1 mM PBS (0.05% SDS) and again with 0.3 M ammonium acetate. The functionalized substrate was kept in PBS buffer (0.3 M Na^+) at room temperature until use. The DNAs used in this study were paired with polyA sequences at the 5′ end before force measurement by annealing at 95 °C for 5 min.

AFM Measurement. Force−distance measurements were performed using a commercial AFM (MFP3D) (for more details, see Supporting Information). The spring constants of the cantilevers were measured using the thermal fluctuation method.[52,53] All measurements were performed at room temperature inside a liquid cell in PBS buffer. The whole system was left to equilibrate for 1 h, with the tip retracted from the surface, before recording force curves. The forces were recorded at different loading rates ranging between 20 and 1500 nm/s starting with *trans*-azobenzene DNA using Asylum research cantilevers (Cr/Au coated BL-RC-150VB). One second dwell time was kept for all measurements to ensure interactions between the tip DNA and the substrate.

Photoswitching of the *trans*-azobenzene DNA was achieved by irradiating the sample with UV light for 3 h using Thorlab M36L2-C3 UV (365 nm) collimated LED for Nikon Eclipse, 700 mA. *cis*-Azobenzene DNA was photoswitched back to *trans* form using a blue LED (Thorlab M470L2-C3 Blue 470 nm, collimated LED for Nikon eclipse, 1600 mA). The intensity of the LED was measured using a calibrated Si photodiode (OSI optoelectronics). We determined the most probable unbinding force by plotting histograms of the rupture forces. The histograms had a bin size of 5, and the threshold was kept between 20 and 150 pN.

Conflict of Interest: The authors declare no competing financial interest.

Acknowledgment. This paper is based on research supported by the Air Force Office of Scientific Research (AFOSR FA9550-10-1-0474).

Supporting Information Available: Figure S1. Cantilevers with different spring constants used to verify the validation Friddle model. Figure S2. Control experiment to test the effect of different photon doses on the decrease in the rupture forces. Figure S3. Fitting parameters used in the Friddle model. Detailed description of the procedure for the force distance measurements. Figure S4. Melting temperature curves of unmodified DNA and azobenzene-modified DNA. Table S1. Melting temperature values extracted from different methods. This material is available free of charge *via* the Internet at http://pubs.acs.org.

REFERENCES AND NOTES

1. Delbruck, M. On the Replication of Desoxyribonucleic Acid (DNA). *Proc. Natl. Acad. Sci. U.S.A.* **1954**, *40*, 783–788.
2. Rosenberg, M.; Court, D. Regulatory Sequences Involved in the Promotion and Termination of RNA-Transcription. *Annu. Rev. Genet.* **1979**, *13*, 319–353.
3. Teles, F. R. R.; Fonseca, L. R. Trends in DNA Biosensors. *Talanta* **2008**, *77*, 606–623.
4. Zhai, J. H.; Cui, H.; Yang, R. F. DNA Based Biosensors. *Biotechnol. Adv.* **1997**, *15*, 43–58.
5. McCullagh, M.; Franco, I.; Ratner, M. A.; Schatz, G. C. DNA-Based Optomechanical Molecular Motor. *J. Am. Chem. Soc.* **2011**, *133*, 3452–3459.
6. Zhang, J.; Ting, B. P.; Jana, N. R.; Gao, Z. Q.; Ying, J. Y. Ultrasensitive Electrochemical DNA Biosensors Based on the Detection of a Highly Characteristic Solid-State Process. *Small* **2009**, *5*, 1414–1417.
7. Campolongo, M. J.; Tan, S. J.; Xu, J. F.; Luo, D. DNA Nanomedicine: Engineering DNA as a Polymer for Therapeutic and Diagnostic Applications. *Adv. Drug Delivery Rev.* **2010**, *62*, 606–616.
8. Vafabakhsh, R.; Ha, T. Extreme Bendability of DNA Less than 100 Base Pairs Long Revealed by Single-Molecule Cyclization. *Science* **2012**, *337*, 1097–1101.
9. Volkov, S. N.; Paramonova, E. V.; Yakubovich, A. V.; Solov'yov, A. V. Micromechanics of Base Pair Unzipping in the DNA Duplex. *J. Phys.: Condens. Matter* **2012**, *24*, 035104.
10. Kafri, Y.; Mukamel, D.; Peliti, L. Melting and Unzipping of DNA. *Eur. Phys. J. B* **2002**, *27*, 135–146.
11. Cocco, S.; Monasson, R.; Marko, J. F. Unzipping Dynamics of Long DNAs. *Phys. Rev. E* **2002**, *66*, 051914.
12. Bockelmann, U.; Thomen, P.; Essevaz-Roulet, B.; Viasnoff, V.; Heslot, F. Unzipping DNA with Optical Tweezers: High Sequence Sensitivity and Force Flips. *Biophys. J.* **2002**, *82*, 1537–1553.
13. Bockelmann, U.; Essevaz-Roulet, B.; Thomen, P.; Heslot, F. Mechanical Opening of DNA by Micro Manipulation and Force Measurements. *C.R. Phys.* **2002**, *3*, 585–594.
14. Wang, M. D.; Yin, H.; Landick, R.; Gelles, J.; Block, S. M. Stretching DNA with Optical Tweezers. *Biophys. J.* **1997**, *72*, 1335–1346.
15. Pope, L. H.; Davies, M. C.; Laughton, C. A.; Roberts, C. J.; Tendler, S. J. B.; Williams, P. M. Force-Induced Melting of a Short DNA Double Helix. *Eur. Biophys. J.* **2001**, *30*, 53–62.
16. Neuman, K. C.; Nagy, A. Single-Molecule Force Spectroscopy: Optical Tweezers, Magnetic Tweezers and Atomic Force Microscopy. *Nat. Methods* **2008**, *5*, 491–505.
17. Asanuma, H.; Ito, T.; Yoshida, T.; Liang, X.; Komiyama, M. Photoregulation of the Formation and Dissociation of a DNA Duplex by Using the *cis*−*trans* Isomerization of Azobenzene. *Angew. Chem., Int. Ed.* **1999**, *38*, 2393–2395.
18. Yamazawa, A.; Liang, X. G.; Asanuma, H.; Komiyama, M. Photoregulation of the DNA Polymerase Reaction by Oligonucleotides Bearing an Azobenzene. *Angew. Chem., Int. Ed.* **2000**, *39*, 2356–2357.
19. Liang, X. G.; Mochizuki, T.; Asanuma, H. A Supra-photoswitch Involving Sandwiched DNA Base Pairs and Azobenzenes for Light-Driven Nanostructures and Nanodevices. *Small* **2009**, *5*, 1761–1768.
20. Liang, X. G.; Takenaka, N.; Nishioka, H.; Asanuma, H. Molecular Design for Reversing the Photoswitching Mode of Turning ON and OFF DNA Hybridization. *Chem.—Asian J.* **2008**, *3*, 553–560.
21. Nishioka, H.; Liang, X. G.; Kato, T.; Asanuma, H. A Photon-Fueled DNA Nanodevice That Contains Two Different Photoswitches. *Angew. Chem., Int. Ed.* **2012**, *51*, 1165–1168.
22. Kang, H. Z.; Liu, H. P.; Phillips, J. A.; Cao, Z. H.; Kim, Y.; Chen, Y.; Yang, Z. Y.; Li, J. W.; Tan, W. H. Single-DNA Molecule Nanomotor Regulated by Photons. *Nano Lett.* **2009**, *9*, 2690–2696.
23. You, M. X.; Chen, Y.; Zhang, X. B.; Liu, H. P.; Wang, R. W.; Wang, K. L.; Williams, K. R.; Tan, W. H. An Autonomous and Controllable Light-Driven DNA Walking Device. *Angew. Chem., Int. Ed.* **2012**, *51*, 2457–2460.
24. Reha, D.; Voityuk, A. A.; Harris, S. A. An *In Silico* Design for a DNA Nanomechanical Switch. *ACS Nano* **2010**, *4*, 5737–5742.
25. Yuan, Q.; Zhang, Y. F.; Chen, T.; Lu, D. Q.; Zhao, Z. L.; Zhang, X. B.; Li, Z. X.; Yan, C. H.; Tan, W. H. Photon-Manipulated Drug Release from a Mesoporous Nanocontainer Controlled by Azobenzene-Modified Nucleic Acid. *ACS Nano* **2012**, *6*, 6337–6344.
26. You, M. X.; Wang, R. W.; Zhang, X. B.; Chen, Y.; Wang, K. L.; Peng, L.; Tan, W. H. Photon-Regulated DNA-Enzymatic Nanostructures by Molecular Assembly. *ACS Nano* **2011**, *5*, 10090–10095.
27. Friedsam, C.; Gaub, H. E.; Netz, R. R. Probing Surfaces with Single-Polymer Atomic Force Microscope Experiments. *Biointerphases* **2006**, *1*, Mr1–Mr21.
28. Albrecht, C.; Blank, K.; Lalic-Multhaler, M.; Hirler, S.; Mai, T.; Gilbert, I.; Schiffmann, S.; Bayer, T.; Clausen-Schaumann, H.; Gaub, H. E. DNA: A Programmable Force Sensor. *Science* **2003**, *301*, 367–370.
29. Kim, E. S.; Kim, J. S.; Lee, Y.; Choi, K. Y.; Park, J. W. Following the DNA Ligation of a Single Duplex Using Atomic Force Microscopy. *ACS Nano* **2012**, *6*, 6108–6114.

30. Sugimoto, Y.; Yurtsever, A.; Abe, M.; Morita, S.; Ondracek, M.; Pou, P.; Perez, R.; Jelinek, P. Role of Tip Chemical Reactivity on Atom Manipulation Process in Dynamic Force Microscopy. *ACS Nano* **2013**, *7*, 7370–7376.
31. Nguyen, T. H.; Steinbock, L. J.; Butt, H. J.; Helm, M.; Berger, R. Measuring Single Small Molecule Binding *via* Rupture Forces of a Split Aptamer. *J. Am. Chem. Soc.* **2011**, *133*, 2025–2027.
32. Claridge, S. A.; Schwartz, J. J.; Weiss, P. S. Electrons, Photons, and Force: Quantitative Single-Molecule Measurements from Physics to Biology. *ACS Nano* **2011**, *5*, 693–729.
33. Frey, E. W.; Gooding, A. A.; Wijeratne, S.; Kiang, C. H. Understanding the Physics of DNA Using Nanoscale Single-Molecule Manipulation. *Front. Phys.* **2012**, *7*, 576–581.
34. Deng, Z.; Lulevich, V.; Liu, F. T.; Liu, G. Y. Applications of Atomic Force Microscopy in Biophysical Chemistry of Cells. *J. Phys. Chem. B* **2010**, *114*, 5971–5982.
35. Sullan, R. M. A.; Churnside, A. B.; Nguyen, D. M.; Bull, M. S.; Perkins, T. T. Atomic Force Microscopy with Sub-picoNewton Force Stability for Biological Applications. *Methods* **2013**, *60*, 131–141.
36. Bell, G. I. Models for the Specific Adhesion of Cells to Cells. *Science* **1978**, *200*, 618–627.
37. Bizzarri, A. R.; Cannistraro, S. The Application of Atomic Force Spectroscopy to the Study of Biological Complexes Undergoing a Biorecognition Process. *Chem. Soc. Rev.* **2010**, *39*, 734–749.
38. Friddle, R. W.; Noy, A.; De Yoreo, J. J. Interpreting the Widespread Nonlinear Force Spectra of Intermolecular Bonds. *Proc. Natl. Acad. Sci. U.S.A.* **2012**, *109*, 13573–13578.
39. Yan, Y. Q.; Chen, J. I. L.; Ginger, D. S. Photoswitchable Oligonucleotide-Modified Gold Nanoparticles: Controlling Hybridization Stringency with Photon Dose. *Nano Lett.* **2012**, *12*, 2530–2536.
40. Yan, Y. Q.; Wang, X.; Chen, J. I. L.; Ginger, D. S. Photoisomerization Quantum Yield of Azobenzene-Modified DNA Depends on Local Sequence. *J. Am. Chem. Soc.* **2013**, *135*, 8382–8387.
41. Beharry, A. A.; Woolley, G. A. Azobenzene Photoswitches for Biomolecules. *Chem. Soc. Rev.* **2011**, *40*, 4422–4437.
42. Strunz, T.; Oroszlan, K.; Schafer, R.; Guntherodt, H. J. Dynamic Force Spectroscopy of Single DNA Molecules. *Proc. Natl. Acad. Sci. U.S.A.* **1999**, *96*, 11277–11282.
43. Lo, Y. S.; Zhu, Y. J.; Beebe, T. P. Loading-Rate Dependence of Individual Ligand-Receptor Bond-Rupture Forces Studied by Atomic Force Microscopy. *Langmuir* **2001**, *17*, 3741–3748.
44. Dudko, O. K.; Filippov, A. E.; Klafter, J.; Urbakh, M. Beyond the Conventional Description of Dynamic Force Spectroscopy of Adhesion Bonds. *Proc. Natl. Acad. Sci. U.S.A.* **2003**, *100*, 11378–11381.
45. Dudko, O. K.; Hummer, G.; Szabo, A. Intrinsic Rates and Activation Free Energies from Single-Molecule Pulling Experiments. *Phys. Rev. Lett.* **2006**, *96*, 108101.
46. Noy, A.; Friddle, R. W. Practical Single Molecule Force Spectroscopy: How To Determine Fundamental Thermodynamic Parameters of Intermolecular Bonds with an Atomic Force Microscope. *Methods* **2013**, *60*, 142–150.
47. Palau, W.; Di Primo, C. Single-Cycle Kinetic Analysis of Ternary DNA Complexes by Surface Plasmon Resonance on a Decaying Surface. *Biochimie* **2012**, *94*, 1891–1899.
48. Mishra, R. K.; Mishra, G.; Li, M. S.; Kumar, S. Effect of Shear Force on the Separation of Double-Stranded DNA. *Phys. Rev. E* **2011**, *84*, 032903.
49. Cocco, S.; Monasson, R.; Marko, J. F. Force and Kinetic Barriers to Unzipping of the DNA Double Helix. *Proc. Natl. Acad. Sci. U.S.A.* **2001**, *98*, 8608–8613.
50. Jin, Q.; Fleming, A. M.; Burrows, C. J.; White, H. S. Unzipping Kinetics of Duplex DNA Containing Oxidized Lesions in an α-Hemolysin Nanopore. *J. Am. Chem. Soc.* **2012**, *134*, 11006–11011.
51. McCullagh, M.; Franco, I.; Ratner, M. A.; Schatz, G. C. Defects in DNA: Lessons from Molecular Motor Design. *J. Phys. Chem. Lett.* **2012**, *3*, 689–693.
52. Hutter, J. L.; Bechhoefer, J. Calibration of Atomic-Force Microscope Tips (Vol 64, Pg 1868, 1993). *Rev. Sci. Instrum.* **1993**, *64*, 3342–3342.
53. Butt, H. J.; Jaschke, M. Calculation of Thermal Noise in Atomic-Force Microscopy. *Nanotechnology* **1995**, *6*, 1–7.